PAPER

Studies on a glutathione coated hollow ZnO modified glassy carbon electrode; a novel Pb(II) selective electrochemical sensor†

Lateef Ahmad Malik, Altaf Hussain Pandith, [iD] * Arshid Bashir, Aaliya Qureashi and Taniya Manzoor

Herein, we report the electrochemical detection of heavy metal ions such as Pb(II), Cd(II) and Hg(II) ions while using glutathione coated hollow ZnO modified glassy carbon electrode (Glu-h-ZnO/GCE). An excellent voltammetric response of the modified electrode towards these metal ions was observed by different voltammetric techniques. Among the different target metal ions, a selective electrochemical response (sensitivity = 4.57 μA μM^{-1}) for the detection of Pb(II) ions was obtained with differential pulse voltammetric (DPV) measurements. Besides, under optimal experimental conditions and in the linear concentration range of 2–18 μM, a very low detection limit of 0.42 μM was obtained for Pb(II) ion. The observed electrochemical behaviour of Glu-h-ZnO/GCE towards these metal ions is in conformity with the band gap of the composite in the presence of various test metal ions. The band gap studies of the composite and various "Composite-Metal Ion" systems were obtained by reflectance as well as by computational methods where results are in close agreement, justifying the observed electrochemical behaviour of the systems. The lowest band gap value of the "Composite-Pb" system may be the reason for the excellent electrochemical response of the Glu-h-ZnO modified GCE towards the detection of Pb(II) ion.

1 Introduction

Heavy metals (HMs) remain persistent in the environment as they cannot be degraded.[1,2] HM ions mainly come from anthropogenic activities such as mining, smelting, or different kinds of wastes. When present in excess, these metal ions accumulate at different tropic levels of the food chain and ultimately result in various diseases and disorders in living beings.[3] Mercury, one of the most toxic heavy metal ions, enters the environment through coal burning, mining or industrial wastes, and is known to cause damage mainly to the nervous system.[4] Lead comes from automobile exhausts, old paints, mining wastes, incinerator ash or water from lead pipes and is

also known to cause damage to the nervous system.[5] Cadmium, which is supposed to cause kidney disorders, comes from the electroplating and mining industries. In view of the severe impacts of heavy metal pollution on the ecosystem, there is an ever-increasing demand for the detection and removal of heavy metal contaminants from aqueous systems.[6–9]

Traditional analytical methods for the detection of heavy metal ions include instrumental analytical techniques such as atomic absorption spectroscopy,[10] atomic emission spectroscopy,[11] inductively coupled plasma mass spectrometry[12] and cold vapour atomic fluorescence spectrometry,[13] which are sensitive but highly expensive and require laborious pretreatment processes.[14] On the other hand electrochemical methods like cyclic voltametry (CV), linear sweep voltammetry (LSV), differential pulse voltammetry (DPV), anodic stripping voltammetry (ASV), Amperometry *etc*, are more cost-effective, time economic, user-friendly, reliable and suitable for in-field applications.[15] These electrochemical techniques possess the advantages like simple procedures and short analytical time as compared to other spectroscopic techniques. Because of the various advantages like good selectivity, portability, low cost, fast analysis speed and excellent sensitivity offered by anodic stripping methods, anodic stripping voltammetry has been widely used for the analysis of heavy metal ions at trace levels.[16–18] In addition to anodic stripping voltammetry, CV and DPV methods are also quite common in the field of metal ion

Laboratory of Nanoscience and Quantum Computations, Department of Chemistry, University of Kashmir, Hazratbal, Srinagar-190006, Kashmir, India. E-mail: altafpandit23@gmail.com; Fax: +91-194-2414049; Tel: +91-194-2424900; +91-7006429021

detection in aqueous samples, besides, being helpful for the detection of some other important metabolites, synthetic anti-oxidants in the vegetable oils, tumor markers *etc.*[19–21] CV has been employed in the selective detection of Hg(ɪɪ) ions using gold nanoparticles-thiol functionalized reduced graphene oxide-modified glassy carbon electrode (GCE/rGO-SH/Au nano-particles) where the low detection limit of 0.2 μM was obtained.[22] In another experiment, a boron-doped diamond film has been used in the detection of Pb(ɪɪ), Cu(ɪɪ) and Hg(ɪɪ) ions[23] while as indium tin oxide (ITO) electrodes modified by gold nanoparticles (Au nanoparticles) have been used in the detection of Hg(ɪɪ) ions using LSV technique.[24] DPV and LSV technique has been used for selective and simultaneous detection of Pb(ɪɪ), Cu(ɪɪ) and Cd(ɪɪ) while using carbon dot-modified electrode as working electrode.[25] Further, because of the various advantages such as being less expensive, easy fabrication, simple operation, sensitivity and least response time offered by modified electrodes,[26–28] they have been successfully used to determine even trace levels of heavy metal ions in electroanalytical chemistry.[29–31] Surface of the electrode has been modified by various electro-active materials such as conducting polymers,[32] graphene,[33] graphene–Au,[22] citrate[34] *etc* for the detection and removal of heavy metal contaminants from aqueous system with promising results. However, ZnO based composite materials have been extensively used in electrochemical sensing applications due to the excellent electrochemical properties.[35]

Here, we report electrochemical detection of heavy metal ions using GCE modified with glutathione coated hollow ZnO previously synthesized in our laboratory.[36] The electrochemical response of modified GCE for the detection of Pb(ɪɪ), Cd(ɪɪ) and Hg(ɪɪ) has been tested by employing CV, DPV and LSV experiments where best response has been observed for the Pb(ɪɪ) ion followed by Hg(ɪɪ) and Cd(ɪɪ) ions. The observed electrochemical response was explained on the basis of variation in band gaps of various "Composite-Metal Ion" systems which were obtained from reflectance and computational methods and the results obtained are in close agreement with the experimental data.

2 Experimental section

2.1 Materials

The materials used in the experimental process are of analytical grade and were used without any further purification and processing. Cadmium nitrate ($Cd(NO_3)_2$), lead nitrate ($Pb(NO_3)_2$), mercuric nitrate ($Hg(NO_3)_2$) and potassium ferricyanide ($K_3[Fe(CN)_6]$), all purchased from Merck Millipore, were used in the electrochemical process. Potassium nitrate (KNO_3), potassium chloride (KCl), hydrochloric acid (HCl) and sulphuric acid (H_2SO_4) used as supporting electrolytes, were purchased from Sigma Aldrich. De-ionised water was used for the washing and as a solvent throughout the experimentation process.

2.2 Synthesis and characterization

2.2.1 Glutathione coated hollow ZnO modified glassy carbon electrode (Glu-h-ZnO/GCE). The complete synthesis and

characterization process of glutathione coated hollow ZnO has been already reported in our previous work.[36]

The modified GCE has been prepared by simple drop casting method. 3 mg of Glu-h-ZnO were dispersed in 10 ml of de-ionized water and was sonicated for 1 hour so as to get the fine suspension of the composite material. With the help of micro pipette, a very small amount of the suspension was drop casted over the cleaned shiny surface of the GCE. The electrode was kept at its position till the composite material on its surface was dried out at room temperature.

2.3 Electrochemical studies

The electrochemical studies of Glu-h-ZnO/GCE for the detection of Pb(ɪɪ), Cd(ɪɪ) and Hg(ɪɪ) ions were carried out with various voltammetric methods. CV and LSV were performed with Knopy tech (K-lyte 1.0) Potentiostat while as DPV measurements have been carried out with Biologic SAS Potentiostate (MP3). The voltammetric measurements of different metal ions of particular concentrations were carried out using Ag/AgCl as reference electrode, Pt mesh as counter electrode and modified GCE as working electrode. In each CV operation for a particular metal ion concentration, corresponding anodic peak currents (I_a) and cathodic peak currents (I_c) were recorded for every forward and backward potential scans, respectively. The peak potential is the characteristics of a particular metal ion while as the magnitude of the peak current is proportional to the concentration of that particular metal ion.

2.4 Diffused reflectance and UV-Vis absorption (DR-UV) studies

Diffused reflectance measurements and solid state UV-Vis absorption spectra of various "Composite-Metal ion" systems were recorded on a Schimadzu-2600 spectrometer using $BaSO_4$ discs and converted to Kubelka–Munk and Tauc plots in plotting software (Origin) using an appropriate conversion formula. The composite material (Glu-h-ZnO) with metal ion of interest adsorbed on it, was washed with de-ionised water and dried in oven at 30 °C which was later used to get absorption and reflectance spectra. From reflectance measurements, the band gap of different composite-metal ion systems were obtained by using Kubelka–Munk function.[37]

2.5 Computational studies

All computational studies pertaining to the electrochemical behaviour of heavy metal ions were carried by density functional theory (DFT) using LanL2DZ and B3LYP as the basis set and functional, respectively. Theoretical UV-Vis absorption spectra of different "Composite-Metal Ion" systems and the corresponding theoretical band gap values were obtained to explain the experimental electrochemical results.

3 Results and discussions

3.1 Electrochemical studies

For the detailed electrochemical analysis of three heavy metal ions *viz.*, Pb(ɪɪ), Hg(ɪɪ) and Cd(ɪɪ) on glutathione coated hollow
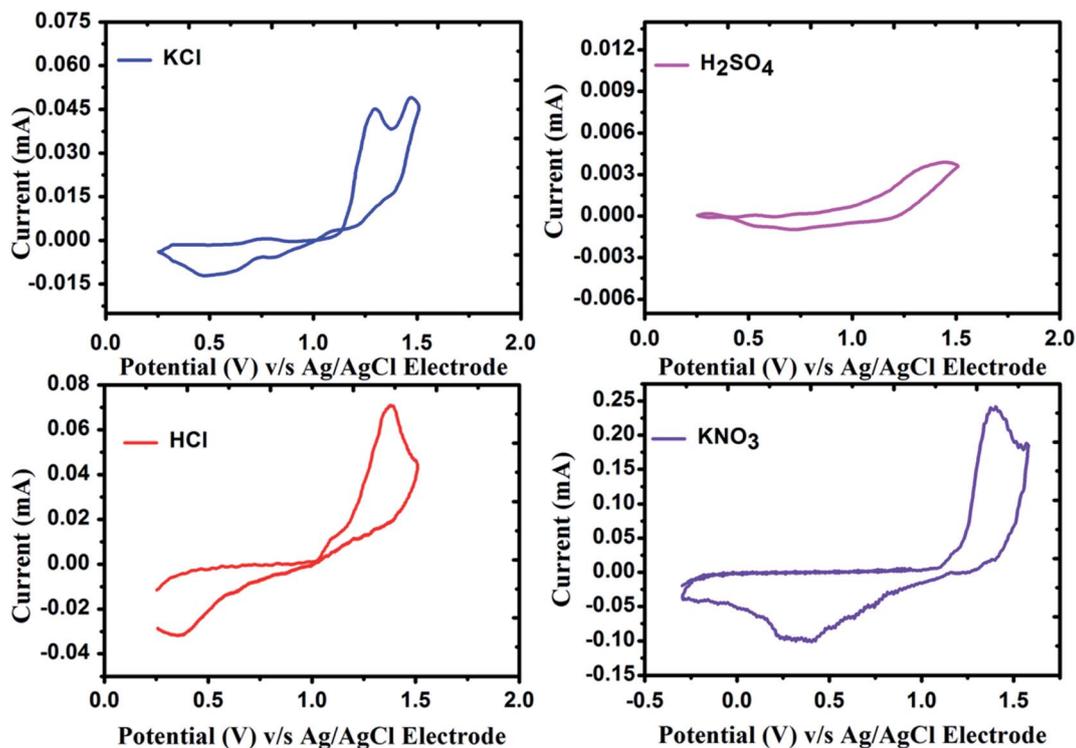
Fig. 1 Cyclic voltammograms of Glu@h-ZnO/GCE for 10^{-3}M Pb(II) solution in various supporting electrolytes using scan rate of 0.05 mV s^{-1} (vs. Ag/AgCl electrode).
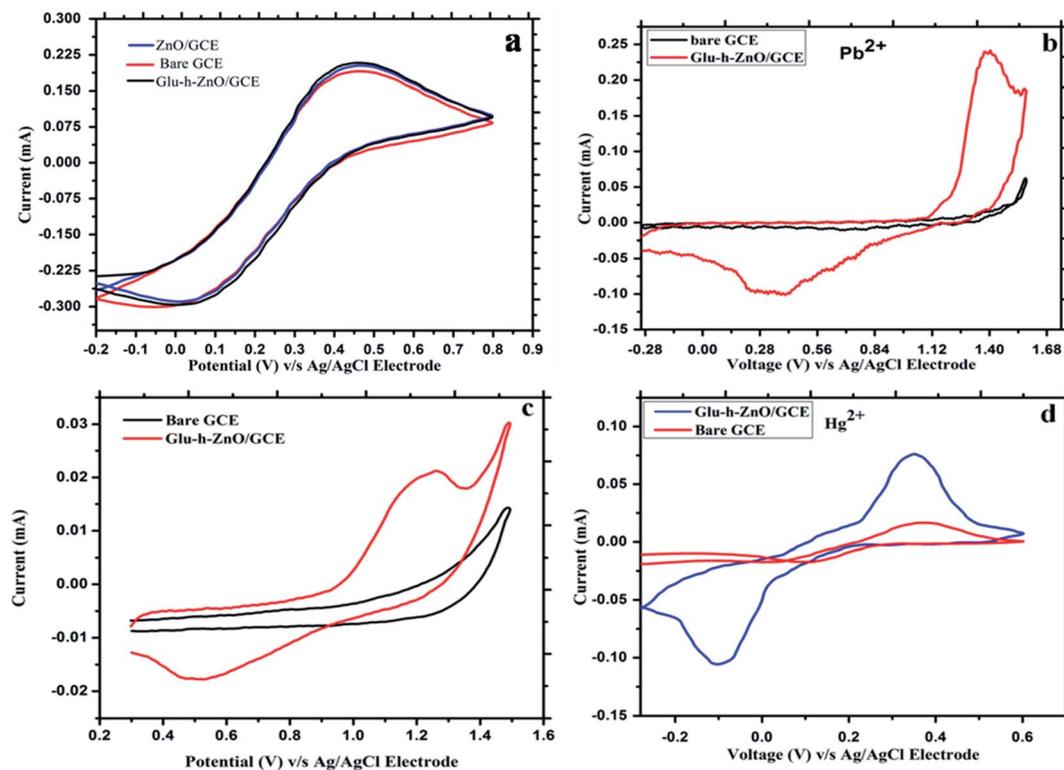

Fig. 2 Cyclic voltammograms of modified/unmodified glassy carbon electrodes for (a) 10^{-3}M aqueous solution of potassium ferrocyanide redox couple, (b) 10^{-3}M Pb(II) solution, (c) 10^{-3}M Cd(II) solution and (d) 10^{-3}M Hg(II) solution in 0.1 M aqueous solution of KNO₃, using scan rate of 0.05 mV s^{-1} (vs. Ag/AgCl electrode).

Table 1 Peak current (anodic and cathodic) and peak potential (anodic and cathodic) values obtained during cyclic voltammetric determination of 10^{-3} M aqueous solutions of Pb(II), Hg(II) and Cd(II) using Glu-h-ZnO/GCE in 0.1 M aqueous solution of KNO_3 at the scan rate of 0.05 mV s^{-1} (vs. Ag/AgCl electrode)

Metal ion	Anodic peak current (I_a) (mA)	Cathodic peak current (I_c) (mA)	Anodic peak potential (Ep$_a$) (V)	Anodic peak potential (Ep$_c$) (V)
Pb(II)	0.240	−0.110	1.285	0.420
Hg(II)	0.075	−0.118	0.38	−0.10
Cd(II)	0.021	−0.017	1.28	0.48

zinc oxide modified glassy carbon electrode, the CV, DPV and LSV measurements were carried out at optimized conditions. In the process of optimization, parameters like optimum scan rate and supporting electrolyte for best electrochemical response were mainly taken into consideration. Cyclic voltammeetric response of the modified electrode for 10^{-3} M Pb(II) ion solution was recorded by varying scan rate from 0.04 mV s^{-1} to 0.10 mV s^{-1}. In the selected range of scan rate, the best response was obtained with the scan rate of 0.05 mV s^{-1} and thus scan rate of 0.05 mV s^{-1} was selected for carrying out all further CV measurements (Fig. S1†). In addition, various electrolytes viz., KCl, KNO_3, HCl and H_2SO_4 as supporting electrolytes were tested to record the electrochemical response of the modified electrode for Pb(II) ion solution. The results indicate that the response varies from almost zero in 0.1 M H_2SO_4 to a maximum in 0.1 M KNO_3 solution (Fig. 1). Keeping this into consideration, 0.1 M KNO_3 was used as supporting electrolyte in all electrochemical studies.

Further, CV measurements of the modified electrode in absence of any metal ion solutions were carried out at optimized conditions in the potential range of −1 V to 1.5 V (Fig. S2†). There is no appearance of any peak in the selected range of potential which indicate that there will be no interference due to the modified electrode while carrying out electrochemical measurements.

3.1.1 Cyclic voltammetric(CV) studies. Cyclic voltammetric measurements of Glu-h-ZnO/GCE, ZnO/GCE and bare GCE were recorded in a solution of 0.1 M potassium ferrocyanide/ferricyanide redox couple at optimized conditions in a potential range of −0.2 V to 0.8 V vs. Ag/AgCl electrode (Fig. 2a).

Although, all the three electrode setup depict almost same level of response in potassium ferrocyanide solution under similar conditions yet a slight better activity is recorded for Glu-h-ZnO/GCE compared to other 2 electrodes cannot be ruled out. When CV measurements of Glu-h-ZnO/GCE and bare GCE were recorded for metal ion solutions, a zero response of bare electrode in comparison to modified electrode for all the three metal ions was observed (Fig. 2b–d). As can be seen from the voltammograms, clear and sharp anodic and cathodic peaks for all the three test metal ions were observed in their selected
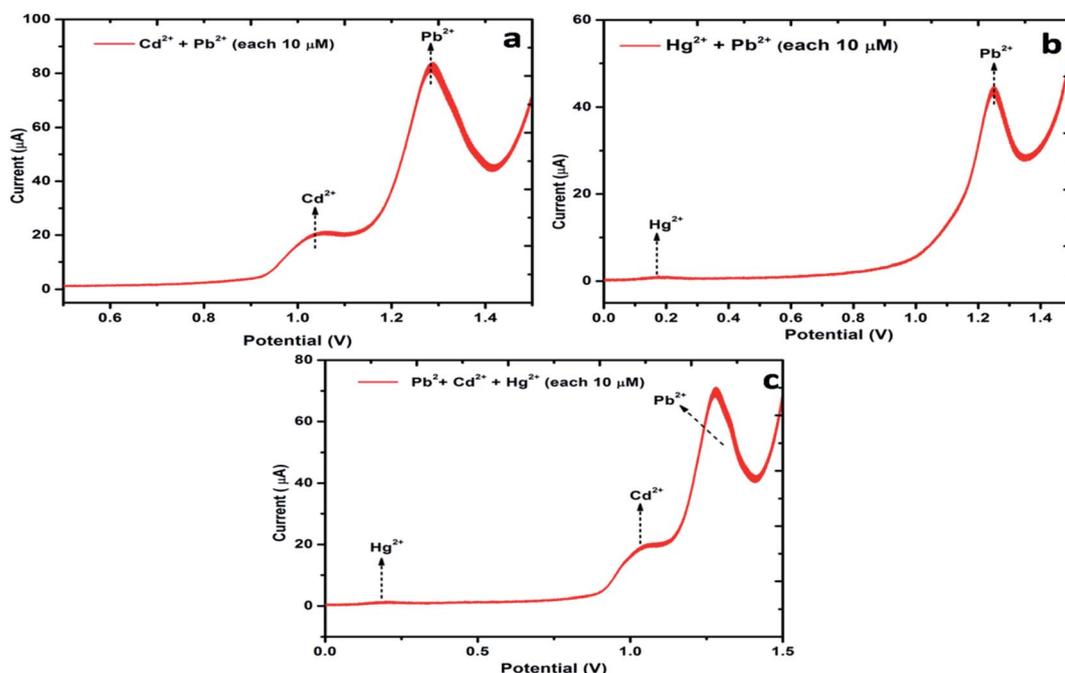

Fig. 3 DPV curves for a solution (a) containing 10 μM Pb(II) and 10 μM Cd(II) ions, (b) containing 10 μM Hg(II) and 10 μM Pb(II) ions and (c) containing 10 μM Pb(II), 10 μM Hg(II) and 10 μM Cd(II) in 0.1 M KNO_3 solution at a scan rate of 100 mV s^{-1}.
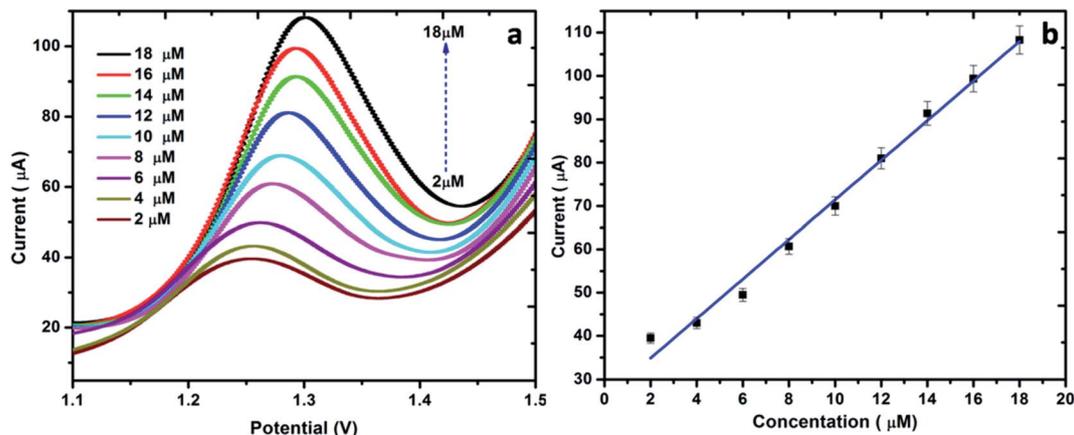
Fig. 4 (a) DPV voltammograms for different concentrations of Pb(II) ion in 0.1 M KNO$_3$ and at a scan rate of 100 mV s^{-1}. (b) The linear relationship between the peak current and the concentration of Pb(II) ion.

potential windows while using modified electrode. The various useful electrochemical parameters obtained from cyclic voltammograms are summarised in the Table 1.

Among all the test metal ions, a highest magnitude of I_a (0.240 mA) and I_c (−0.110 mA), was obtained for the Pb(II) ion and lowest magnitude of I_a(0.021 mA) and I_c (−0.017 mA) was observed for Cd(II) ion. As it is well known that the I_a and I_c values are representative indices of the oxidation and reduction potential of the metal ions, respectively; therefore these results indicate that significantly a better electrochemical activity is taking place between Pb(II) ion and electrode surface in comparison to Hg(II) and Cd(II) ions. A better understanding of the observed electrochemical behaviour of test metal ions on the electrode surface has been provided by DFT and solid state DR-UV studies on band gap variations in different "Composite-Metal" systems.

3.1.2 Linear sweep and differential pulse voltammetric studies. LSV and DPV measurements were carried out to have an understanding of the selective response behaviour, limit of detection and sensitivity of the modified electrode towards the selected metal ions. The details about LSV measurements have

been provided in the ESI† (S3). DPV measurements were carried out with equimolar (10 μM) solutions of different metal ions. The corresponding voltammograms recorded for Pb–Hg, Cd–Hg and Pb–Cd–Hg systems indicate that the electrochemical response of Pb(II) ion is much higher compared to other two in different ion mixtures, suggesting that the modified electrode is selectively sensing the presence of Pb(II) ion in a mixture (Fig. 3). From the earlier studies,[38] it has been reported that adsorption affinity of modified/GCE for a particular metal ion is a driving force in determining its selective response during electrochemical studies. In our previous study, we have established that Glu-h-ZnO is possessing highest affinity for Hg(II) ion compared to Pb(II) and Cd(II) ions.[36] On contrary to the adsorption behavior, the modified/GCE is showing highest electrochemical response for the Pb(II) ion in comparison to Hg(II) and Cd(II) ions. However, previous adsorption studies indicate that the adsorption affinities of the three selected metal ions for Glu-h-ZnO do not show much variations and from the solid state DR-UV studies, it was observed that the band gap of the composite changes after metal ion adsorption. To explain the observed electrochemical response, it may be

Table 2 A comparison (in terms of LOD and linear concentration range) between different modified electrodes in detection of Pb(II) ions by different voltammetric techniques

| Modified Electrode	Electrochemical technique	Limit of detection	Linear concentration range	Reference
Fe$_3$O$_4$@PANI nanocomposites	Anodic stripping voltammetry	0.0001–10 μM	0.03 nM	39
L-Cysteine tungstophosphate-modified polycrystalline gold electrode (Au-(Cys)PW)	Square wave anodic stripping	0.01–0.2 μM	4.0 nM	40
Fe$_3$O$_4$/Bi$_2$O$_3$/C$_3$N$_4$-modified glassy carbon electrode (GCE)	Square wave anodic stripping	0.01–3.0 μM	0.001 μM	41
Carbon nanotubes functionalized CoMn$_2$O$_4$ nanocomposite	Square wave anodic stripping	0.01–0.85 μM	0.004 μM	42
Glutathione-coated hollow ZnO modified glassy carbon electrode	Differential pulse voltammetry	2–18 μM	0.42 μM	This work
Reduced graphene oxide (RGO) and gold nanoparticles (AuNPs)	Differential pulse voltammetry	0.00005–400 μM	0.015 nM	43
An ionic liquid supported CeO$_2$ nanoparticles–carbon nanotubes composite	Differential pulse voltammetry	0.01 μM–10 μM	5 nM	44
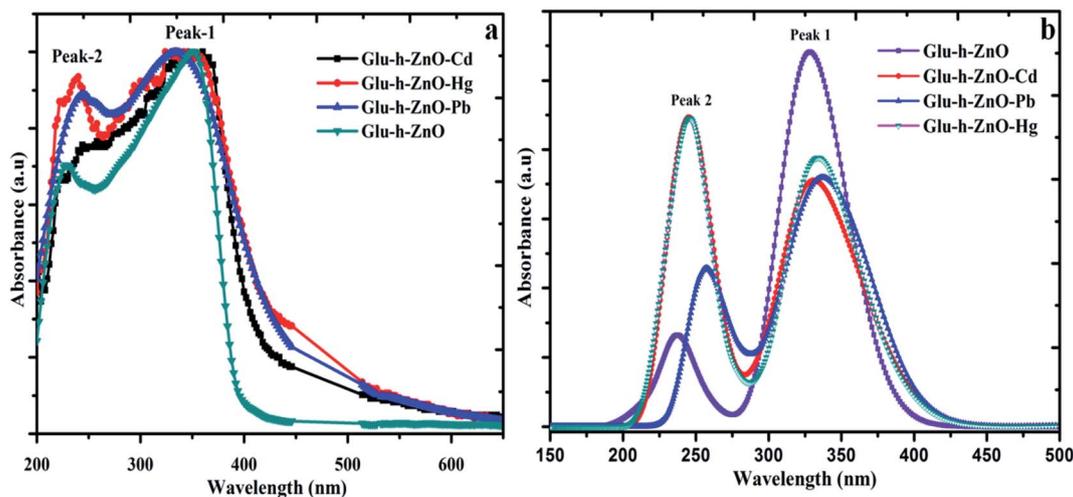
Fig. 5 (a) Experimental (solid state) UV-Vis absorption spectra (b) simulated UV-Vis absorption spectra of Glu-h-ZnO and various "Glu-h-ZnO-Metal Ion" systems (using DFT).

considered that both adsorption affinity as well as band gap factor together may be responsible for controlling the overall electronation process. Owing to the lowest band gap of Composite-Pb(II) system, the electronation process involved in the detection of Pb(II) ion is very much feasible in comparison to Hg(II) and Cd(II), resulting in the selective response of Pb(II) ion.

In order to obtain the sensitivity and limit of detection of the modified electrode for Pb(II) ion, DPV measurements for the different concentrations of Pb(II) solutions (2 μM–18 μM) were carried out at optimized conditions and the corresponding voltammograms were recorded as shown in the Fig. 4a.

With the increase in the concentration of Pb(II) ion, there is a steady increase in the corresponding peak currents. Peak current was found to vary linearly with the Pb(II) ion concentration in a concentration range of 2–18 μM, with correlation coefficient very close to unity ($R^2 = 0.9901$). The sensitivity of the
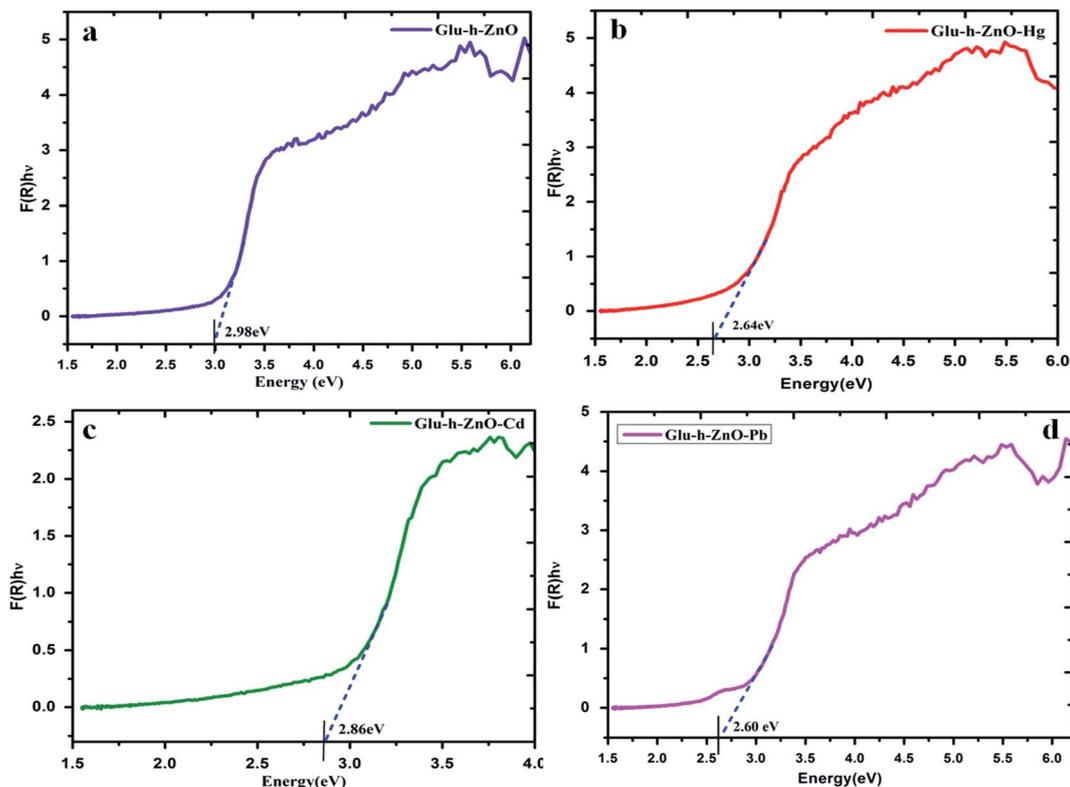

Fig. 6 Tauc plots obtained from the solid state defused reflectance (DR) measurements for determination of optical band gap values of various "Composite-Metal Ion" systems; (a) Glu-h-ZnO, (b) Glu-h-ZnO–Hg(II) (c) Glu-h-ZnO–Cd(II) and (d) Glu-h-ZnO–Pb(II).

Table 3 Theoretical and experimental band gap values of Glu-h-ZnO and various "Glu-h-ZnO–Metal Ion" systems

System	Theoretical band gap (eV)	Experimental band gap (eV)
Glu-h-ZnO	3.762	2.98
Glu-h-ZnO–Cd(II)	2.738	2.86
Glu-h-ZnO–Hg(II)	2.558	2.64
Glu-h-ZnO–Pb(II)	2.345	2.60

electrode for the Pb(II) ion was found to be 4.57 µA µM^{-1} which was obtained from the slope of the current–concentration plot (Fig. 4b). Besides, a very low limit of detection (LOD = 0.42 µM) for Pb(II) was obtained (3σ method) which is quite good for this electrode when compared to other modified electrodes for the detection of Pb(II) ions from aqueous systems (Table 2).

3.2 Diffuse reflectance and solid state absorption (DR-UV) studies

Solid state Reflectance (DR) and UV-Vis adsorption studies of different "Composite-Metal Ion" systems were carried out to study the influence of these metal ions in tuning the band gap of the composite in comparison to the nascent composite system. The UV-Vis absorption spectra of these systems depict two peaks, one at around 380 nm (peak 1) and another peak in the range of 240–270 nm (peak 2). There is not much appreciable shift in the peak positions of the "Composite-Metal" systems in comparison to pure composite for the peak 1 (Fig. 5a).

However, in case of peak 2, a prominent red shift with respect to the pure composite is clearly visible in the absorption spectra. The red shift in the "Composite-Metal" systems is the indication that the adsorbed metal ion is actively taking part in tuning the energy bands of the composite which has been further confirmed from present DFT studies. In order to get the further evidence regarding the influence of metal ions on the band structure, solid state reflectance measurements were carried out. From the reflectance data, the band gap of various "Composite-Metal" systems was calculated and their Tauc plots are shown in (Fig. 6).

The band gap results obtained are in close conformity to the observed absorption spectra and the lowering of the band gap value was observed in "Composite-Metal" systems in comparison to pure composite (Table 3).

The band gap, which is lowest for "Composite-Pb(II)" system followed by Cd(II) and Hg(II) systems, is in accordance with the red shift observed in the UV-Vis absorption spectra. The experimental band gap values were correlated with the theoretical values obtained from DFT studies discussed in the following section.

3.3 Theoretical studies

To have a deeper knowledge about the HOMO–LUMO band structure of Glu-h-ZnO and the changes occurring in the band gap by the influence of adsorbed metal ions, theoretical studies of "Composite-Metal" systems were carried out using density functional theory. DFT studies in terms of UV-Vis absorption
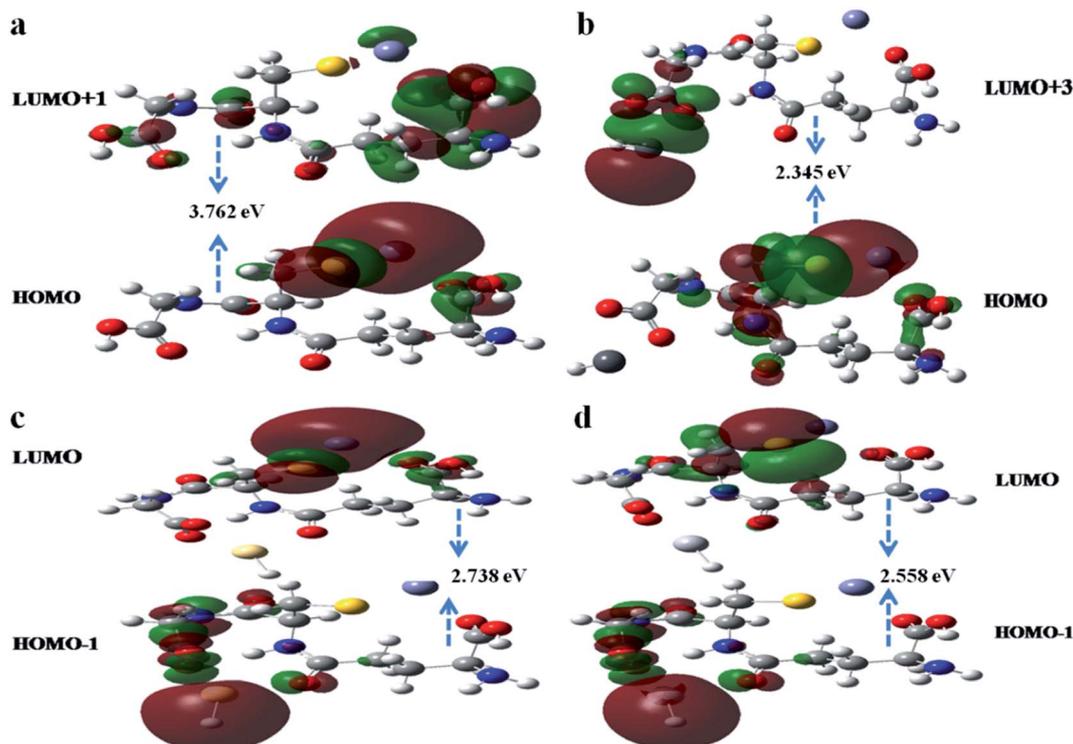

Fig. 7 Frontier Molecular Orbital (FMO) pictures of HOMO and LUMO involved in the main transitions in (a) Glu-h-ZnO composite, (b) Glu-h-ZnO–Pb(II), (c) Glu-h-ZnO–Hg(II), and (d) Glu-h-ZnO–Cd(II) systems.

spectra, Frontier Molecular Orbital (FMO) pictures of HOMO and LUMO actively involved in the main transitions of the electronic spectra and the theoretical band gaps of selected "Composite-Metal" systems were obtained to support the experimental results. Though, the theoretically obtained band gaps are slightly greater than experimental ones, a close agreement in order and overall electronic spectra was obtained between the theoretical and experimental results. Like experimental, the theoretical UV-Vis spectra of Glu-h-ZnO-metal systems also indicate two well resolved peaks in the UV region for each "Composite-Metal" system (Fig. 5b). Like experimental UV-Vis spectra, the theoretical spectra also indicate shift in the peak positions for peak 2 in the wave length range of 230 nm to 270 nm. The shift towards higher wave length with respect to pure composite was observed for "Composite-Metal" systems in the order of Glu-h-ZnO–Pb(II) > Glu-h-ZnO–Cd(II) = Glu-h-ZnO–Hg(II) > Glu-h-ZnO. Such a red shift in "Composite-Metal" systems indicates that the approaching metal ions tune the band gap of the composite to a larger extent after being adsorbed on the composite. This observation is again proved by calculating the theoretical band gaps of such systems where lower band gaps of "Composite-Metal" systems were obtained in comparison to the Glu-h-ZnO (Table 3). To further investigate the involvement of the metal ions in tuning the band gap of the composite, the FMOs pictures of HOMO and LUMO were analysed (Fig. 7).

The contribution of adsorbed metal ions in defining HOMO or LUMO of the composite is clearly observed from their FMO pictures. Among these metal ions, contribution of Pb(II) ion towards HOMO–LUMO is maximum compared to Cd(II) and Hg(II) ions which may be the reason for lowest band gap in "Composite-Pb(II)" system. The adsorbed lead ion is actively involved in defining the LUMO of the Pb(II)-composite system with full contribution indicating that there will be more facile electron transfer from the composite to Pb(II) ions as compared to other systems. All these theoretical studies in the form of UV-Vis spectra, band gap calculations and FMO pictures of HOMO–LUMO systems, provide a valid justification of the observed electrochemical behaviour of Glu-h-ZnO/GCE for the detection of Pb(II), Cd(II) and Hg(II) ions where best electrochemical behaviour was observed for the detection of Pb(II) ion.

4 Conclusions

Glutathione coated hollow zinc oxide (Glu-h-ZnO) previously reported by our research group, exhibited excellent heavy metal ion adsorption properties. Now the same composite material has been used as a selective electrochemical sensor for Pb(II) ion. The electrochemical properties of Glu-h-ZnO/GCE were explored with CV, LSV and DPV like techniques and the results indicate that there is a highest and selective response of the modified electrode for Pb(II) ions as compared to other two metal ions. The sensitivity of the modified electrode for Pb(II) ion has been found to be 4.57 $\mu A \mu M^{-1}$ and can detect Pb(II) ion even at very low concentrations (LOD = 0.42 μM). The observed electrochemical behaviour of the composite material was justified by solid state UV experiments and DFT calculations in

terms of band gap studies of various "Composite-Metal" systems. Highest electrochemical response of Glu-h-ZnO for Pb(II) ion is attributed to the lowest band gap observed for the "Composite-Pb(II)" system which results in feasible electron transfer from composite to metal ion and *vice versa*.

Conflicts of interest

There are no conflicts to declare.

Acknowledgements

Notes and references

1 L. A. Malik, A. Bashir, N. Ahmad, A. Qureashi and A. H. Pandith, *Chemistry Select*, 2020, **5**, 3208.
2 A. Bashir, L. A. Malik, S. Ahad, T. Manzoor, M. A. Bhat, G. N. Dar and A. H. Pandith, *Environ. Chem. Lett.*, 2019, **17**, 729.
3 H. Ali and E. Khan, *Environ. Chem. Lett.*, 2018, **16**, 903.
4 T. Wajima and K. Sugawara, *Fuel Process. Technol.*, 2011, **92**, 1322.
5 G. Flora, D. Gupta and A. Tiwari, *Interdiscip. Toxicol.*, 2012, **5**, 47.
6 A. Bashir, S. Ahad and A. H. Pandith, *Ind. Eng. Chem. Res.*, 2016, **55**, 4820.
7 L. A. Malik, A. Bashir, A. Qureashi and A. H. Pandith, *Environ. Chem. Lett.*, 2019, **17**, 1495.
8 A. Bashir, S. Ahad, L. A. Malik, T. Manzoor, A. Qureashi, G. N. Dar and A. H. Pandith, *Ind. Eng. Chem. Res.*, 2021, **59**, 22353–22397.
9 A. Bashir, T. Manzoor, L. A. Malik, A. Qureashi and A. H. Pandith, *ACS Omega*, 2020, **5**, 4853–4867.
10 T. Gong, J. Liu, X. Liu, J. Liu, J. Xiang and Y. Wu, *Food Chem.*, 2016, **213**, 306.
11 G. Array and A. Merkoci, *Electrochim. Acta*, 2012, **84**, 49.
12 H. Wang, Z. K. Wu, B. B. Chen, M. He and B. Hu, *Analyst*, 2015, **140**, 5619.
13 A. Lebedev, N. Sinikova, S. Nikolaeva, O. Poliakova, M. Khrushcheva and S. Pozdnyakov, *Environ. Chem. Lett.*, 2003, **1**, 107.
14 C. F Harrington, R. Clough, L. R. Drennan-Harris, S. J. Hill and J. F. Tyson, *J. Anal. At. Spectrom.*, 2011, **26**, 1561.
15 C. Zhu, G. Yang, H. Li, D. Du and Y. Lin, *Anal. Chem.*, 2015, **87**, 230.
16 Y. H. Zhu, J. Hu and J. L. Wang, *J. Hazard. Mater.*, 2012, **221**, 155.
17 Q. X. Zhang, H. Wen, D. Peng, Q. Fu and X. J. Huang, *J. Electroanal. Chem.*, 2015, **739**, 89.

18 X. Yao, Z. Guo, Q. Yuan, Z. Liu, J. Liu and X. Huang, *ACS Appl. Mater. Interfaces*, 2014, **6**, 12203.

19 J. Hao, K. Wu, C. Wan and Y. Tang, *Talanta*, 2018, **185**, 550.

20 T. Gan, A. Zhao, S. Wang, Z. Lv and J. Sun, *Sens. Actuators, B*, 2016, **235**, 707.

21 J. Hao, C. Li, K. Wu, C. Hu and N. Yang, *ACS Appl. Nano Mater.*, 2019, **2**, 7747.

22 N. R. Devi, M. Sasidharan and A. K. Sundramoorthy, *J. Electrochem. Soc.*, 2018, **165**, 3046.

23 E. Nurhayati, Y. Juang, M. Rajkumar, C. Huang and C. Hu, *Sep. Purif. Technol.*, 2015, **156**, 1047.

24 N. Ratner and D. Mandler, *Anal. Chem.*, 2015, **87**, 5148.

25 M. Y. Pudza, Z. Z. Abidin, S. Abdul-Rashid, F. M. Yasin, A. S. M. Noor and J. Abdullah, *Environ. Sci. Pollut. Res.*, 2020, **27**, 13315.

26 M. Sajid, M. K. Nazal, M. Mansha, A. Alsharaa, S. M. S. Jillani and C. Basheer, *Trends Anal. Chem.*, 2016, **76**, 15.

27 Y. Li, J. Du, J. Yang, D. Liu and X. Lu, *Colloids Surf., B*, 2012, **97**, 32.

28 D. P. Quan, D. P. Tuyen, T. D. Lam, P. T. N. Tram, N. H. Binh and P. H. Viet, *Colloids Surf., B*, 2011, **88**, 764.

29 K. M. Hassan, G. M. Elhaddad and M. A. Azzem, *Microchim. Acta*, 2019, **186**, 440.

30 W. Wu, M. Jia, Z. Wang, W. Zhang, Q. Zhang, G. Liu, Z. Zhang and P. Li, *Microchim. Acta*, 2019, **186**, 97.

31 T. Kokab, A. Shah, F. J. Iftikhar, J. Nisar, M. S. Akhter and S. B. Khan, *ACS Omega*, 2019, **4**, 22057.

32 Z. Wang, E. Liu and X. Zhao, *Thin Solid Films*, 2011, **519**, 5285.

33 S. Sang, D. Li, H. Zhang, Y. Sun, A. Jian, Q. Zhang and W. Zhang, *RSC Adv.*, 2017, **7**, 21618.

34 A. Qureashi, A. H. Pandith, A. Bashir, T. Manzoor, L. A. Malik and F. A. Sheikh, *Surf. Interfaces*, 2021, **23**, DOI: 10.1016/j.surfin.2021.101004.

35 J. Hao, L. Ji, K. Wu and N. Yang, *Carbon*, 2018, **130**, 480.

36 L. A. Malik, A. Bashir, T. Manzoor and A. H. Pandith, *RSC Adv.*, 2019, **9**, 15976.

37 A. A. Dar and A. A. Ganie, *Cryst. Growth Des.*, 2020, **20**, 3888.

38 Z. Zhao, X. Chen, Q. Yang, J. Liu and X. Huang, *Chem. Commun.*, 2012, **48**, 2180.

39 Y. Kong, T. Wu, D. Wu, Y. Zhang, Y. Wang, B. Du and Q. Wei, *Anal. Methods*, 2018, **10**, 4784.

40 S. Dianat, A. Hatefi-Mehrajdi, K. Mahmoodzadeh and S. Kakhki, *New J. Chem.*, 2019, **43**, 14417.

41 Y. Pu, Y. Wu, Z. Yu, L. Lu and X. Wang, *Talanta*, 2021, **3**, 100024.

42 N. Bashir, M. Akhtar, H. Z. R. Nawaz, D. M. I. Warsi, D. I. Shakir, D. P. O. Agboola and D. S. Zulfiqar, *Chemistry Select*, 2020, **5**, 7909.

43 C. Lai, Y. Zhang, X. Liu, S. Liu, B. Li, M. Zhang, L. Qin, H. Yi, M. Li, Y. Fu, J. He and L. Chen, *Anal. Bioanal. Chem.*, 2019, **411**, 7499.

44 Y. Lia, X. Liua, X. Ninga, C. Huanga, J. Zhenga and J. Zhang, *J. Pharm. Anal.*, 2011, **1**, 258.